DALTON

Structural studies of polyoxometalate-anion-pillared layered double hydroxides †

John Evans,* Martyn Pillinger and Jingjing Zhang

Department of Chemistry, University of Southampton, Southampton SO17 1BJ, UK

New examples of polyoxometalate-anion-pillared layered double hydroxides have been prepared by ion exchange and direct synthesis methods and characterised by powder X-ray diffraction, extended X-ray absorption fine structure (EXAFS), IR and UV/VIS spectroscopy. Complete conversion into crystalline phases was achieved by reaction at pH 4–12 of wet MgAl[Cl^-] or ZnAl[NO_3^-] layered double hydroxide precursors with the species $Nb_xW_{6-x}O_{19}^{(x+2)-}$ (x = 2–4), $[V_2W_4O_{19}]^{4-}$, $[V_{10}O_{28}]^{6-}$, $[Ti_2W_{10}PO_{40}]^{7-}$ and $[NaP_5W_{30}O_{110}]^{14-}$; MgAl[$V_2W_4O_{19}^{4-}$] was also formed *via* MgAl[Br^-] in dichloromethane–ethanol. The hexametalate ions in MgAl[$M_6O_{19}^{n-}$] orient themselves with their shortest dimensions (C_3 axis) perpendicular to the host layers (d_{003} 12.0–12.5 Å) whereas in ZnAl[$NaP_5W_{30}O_{110}^{14-}$] the ion is oriented with its shortest dimension (C_5 axis) parallel to the host layers (d_{003} 21 Å). The structures of several of these incorporated clusters have been verified unequivocally by obtaining tungsten L_{III}-edge and niobium K-edge EXAFS data for the pillared derivatives and pure salts. The layered double hydroxide intercalates MgAl[$Nb_4W_2O_{19}^{6-}$], ZnAl[$Ti_2W_{10}PO_{40}^{7-}$] and ZnAl[$NaP_5W_{30}O_{110}^{14-}$] were also prepared by a direct coprecipitation procedure. In the third synthetic strategy, ZnCr[$V_{10}O_{28}^{6-}$], NiAl[$V_2W_4O_{19}^{4-}$] and ZnAl[$XW_{12}O_{40}^{n-}$] (X = B or Si) layered double hydroxides were obtained *via* directly synthesised terephthalate-, 4-methylbenzoate- and 4-hydroxybenzoate-anion-pillared precursors respectively. 4-Methylbenzoate intercalates were found to be the best precursors out of a series of benzenecarboxylate anion-pillared layered double hydroxides investigated. Zinc, chromium and nickel K-edge EXAFS data in addition to UV/VIS spectroscopic data for the ZnCr and NiAl materials indicate that no significant disruption occurred in the layer structures during ion exchange.

The incorporation of inorganic polymeric species into the interlayers of two-dimensional materials has for some time been investigated as a route to molecular sieve-type compounds that mimic the zeolite-type structure but possess larger and more modifiable pores and active sites.[1] The pillaring of layered double hydroxides by polyoxometalates is one area of interest that has attracted considerable attention over the last eight years or so.[2–15] These materials are complementary to layered silicate clays (smectite clays) intercalated by polyoxocations, for example the Keggin[16] ion $[Al_{13}O_4(OH)_{24}(H_2O)_{12}]^{7+}$, which have been shown to be thermally stable precursors to microporous catalysts. Hydrotalcite-like layered double hydroxides belong to the pyroaurite-sjögrenite group of clay minerals and have the general composition $[M^{2+}{}_{1-x}M^{3+}{}_x(OH)_2][X^{n-}]_{x/n}\cdot zH_2O$,[17] abbreviated $M^{II}{}_rM^{III}[X^{n-}]$ where $r = (1-x)/x$. Their structure consists of positively charged brucite-like sheets separated by charge-balancing anions and water molecules. The layer charge densities are relatively high ($\geqslant$0.04 e Å^{-2} compared to *ca.* 0.01 e Å^{-2} for smectites) and therefore suitable pillaring agents must have large charge densities in order to prevent overcrowding of the galleries. Many of the early transition-metal polyoxoanions meet this requirement. They are also thermally robust and have a wide field of applications, for example as acid catalysts and oxidation catalysts.[18] A patent in 1984 referred to the use of polyoxometalate layered double hydroxides as exhaust gas and hydrocarbon conversion catalysts.[3] More recently, Tatsumi *et al.*[4] showed that hydrotalcite pillared by $[Mo_7O_{24}]^{6-}$ and $[W_{12}O_{41}]^{10-}$ catalysed the epoxidation of alkenes with significant shape selectivity.

Pinnavaia and co-workers[2,5] showed in early reports that the layer double hydroxides $Zn_2Al[X]$, $Zn_2Cr[X]$ and $Ni_3Al[X]$ (X = Cl^- or NO_3^-) could undergo facile and complete exchange with aqueous solutions of $[NH_4]_6[V_{10}O_{28}]$ at pH 4.5, α-$[H_2W_{12}O_{40}]^{6-}$ and α-$[SiV_3W_9O_{40}]^{7-}$ to give pillared derivatives with basal spacings of 11.9 and 14.5 Å. Similar direct pillaring reactions of Mg_rAl, Ni_rAl and Zn_rAl layered double hydroxides with the Keggin-type anions $H_xV_nW_{12-n}O_{40}^{(x-3-n)}$ (n = 2–4) have also been reported.[6] Drezdon[7] synthesised the layered double hydroxide intercalates $Mg_2Al[V_{10}O_{28}^{6-}]$ and $Mg_2Al[Mo_7O_{24}^{6-}]$ *via* a terephthalate-anion-pillared precursor in order to avoid the problems associated with exchanging a small ion such as chloride with a large polyoxoanion. These materials produced both propylene and acetone when screened for propan-2-ol conversion activity, indicating the presence of both acidic and basic catalyst sites. Polyoxometalate layered double hydroxides with the same composition have also been formed by slurrying calcined $Mg_rAl[CO_3^{2-}]$ in carbonate-free $[VO_3]^-$ or $[Mo_7O_{24}]^{6-}$ solutions followed by acidification to pH 4.5.[8] Recent papers by Ulibarri and co-workers[9,10] present studies of the synthesis and properties of vanadate-exchanged layered double hydroxides. Dimotakis and Pinnavaia[11] synthesised an adipate-anion-pillared layered double hydroxide at ambient temperature by reaction of a synthetic meixnerite analogue, of composition $[Mg_3Al(OH)_8][OH]\cdot 2H_2O$, with a glycerol–water–adipic acid mixture (glycerol acting as swelling agent). Aqueous ion exchange of the adipate ion with $[H_2W_{12}O_{40}]^{6-}$ or $[SiW_{11}O_{39}]^{8-}$ in the presence of glycerol then gave polyoxometalate layered double hydroxides. Pinnavaia and co-workers[12] have also reported the coprecipitation of Zn^{2+} and Al^{3+} ions in moderately acidic α-$[SiW_{11}O_{39}]^{8-}$ solution to give a pillared phase with an exceptionally well ordered gallery height of 9.8 Å.

Physical techniques used to characterise polyoxometalate layered double hydroxides have included powder X-ray diffraction (XRD), IR and Raman[13] spectroscopy, Brunauer–Emmett–Teller (BET) (N_2) surface area and porosity measurements, ^{51}V magic angle spinning (MAS) NMR spectroscopy[2] and electron spin resonance spectroscopy.[14] We

† *Non-SI units employed:* eV $\approx$ 1.60 $\times$ 10^{-19} J, Torr $\approx$ 133 Pa.

have previously shown that X-ray absorption fine structure (XAFS) spectroscopy may be used to characterise the co-ordination centres present upon transformation of chromia pillared smectite clays to active methanol dehydration catalysts.[19] There have only been a few reports concerned with XAFS studies of hydrotalcite-like clays.[13,15,20-21] In 1983 De Roy *et al.*[20] investigated the structure of a $Zn_2Cr[Br^-]$ layered double hydroxide using X-ray absorption near-edge structure (XANES) and extended X-ray absorption fine structure (EXAFS) analysis of the K-edge spectra of chromium, zinc and bromine. Their results indicated octahedral co-ordination for chromium and zinc and a delocalisation of the bromide ion. Rives *et al.*[21] carried out a similar study on a novel $Mg_{2.45}V[CO_3^{2-}]$ layered double hydroxide. The low intensity of the pre-edge peak at 5468 eV in the normalised vanadium K-edge XANES spectrum confirmed that most of the vanadium ions were in the +3 oxidation state. Analysis of the vanadium K-edge EXAFS revealed one shell of six oxygens at 2.04 Å and a further shell at *ca.* 3.0 Å associated with vanadium and/or magnesium ions within the layers. Doeuff *et al.*[15] obtained zinc K-edge EXAFS data for a $Zn_2Al[NO_3^-]$–$[V_{10}O_{28}^{6-}]$ system to show that the layered double hydroxide host remained intact during the pillaring reaction.

In this paper we present structural studies of new polyoxometalate layered double hydroxides prepared by ion-exchange reactions of chloride- or nitrate-ion-containing precursors, direct coprecipitation methods and ion-exchange reactions of benzenecarboxylate-ion-pillared precursors. Synthetic conditions have been optimised and the relative merits of each method will be discussed. The characterisation of several of these materials has been advanced by obtaining EXAFS data for both the elements of the host lattice (zinc, chromium and nickel K edges) and those of the incorporated clusters (niobium K and tungsten L_{III} edges). The application of EXAFS spectroscopy to the study of polyoxometalates has been described in the preceding paper.[22]

Results and Discussion

Synthesis of polyoxometalate layered double hydroxides *via* small-ion-containing precursors

The starting materials, abbreviated $M^{II}Al^{III}[X^{n-}]$, were prepared using standard coprecipitation methods with special attention paid to avoiding carbonate interference. Aging of the precipitates at 95 °C (1 week) for $MgAl[X^{n-}]$ and 85 °C (18 h) for $ZnAl[NO_3^-]$ resulted in XRD patterns characteristic of well crystallised hydrotalcite-like minerals with basal spacings (d_{003}) of 7.88, 8.97 and 8.93 Å for $MgAl[Cl^-]$ [Fig. 1(*a*)], $MgAl[NO_3^-]$ and $ZnAl[NO_3^-]$ respectively. Ion-exchange reactions were then carried out with a series of polyoxometalates at a pH between 4 and 12 depending on the polyanion and the layered double hydroxide cations, typically with a temperature of 80 °C, time of 1 h, and molar excess of polyoxometalate of about 50% (Table 1). Complete or close to stoichiometric uptake was achieved in all cases on the basis of IR, XRD, EDX (energy dispersive X-ray) analysis and yield calculations. The best results were obtained when the precursor clays were not dried but stored as aqueous dispersions since the intercalation of water into the interlayer clearly assists swelling in the *z* direction.[6] There should also be pH compatibility between the host and guest species in order to avoid hydrolysis side reactions, either of the layered double hydroxide (*e.g.* dissolution of basic divalent cations from the layers under acidic conditions) or of the polyoxometalate (decomposition of acidic anions under basic conditions). For example, the niobotungstates $[Nb_3W_3O_{19}]^{5-}$ and $[Nb_4W_2O_{19}]^{6-}$ are hydrolytically stable in the zones 5.5 < pH < 11.5 and 8.5 < pH respectively and are therefore ideally compatible

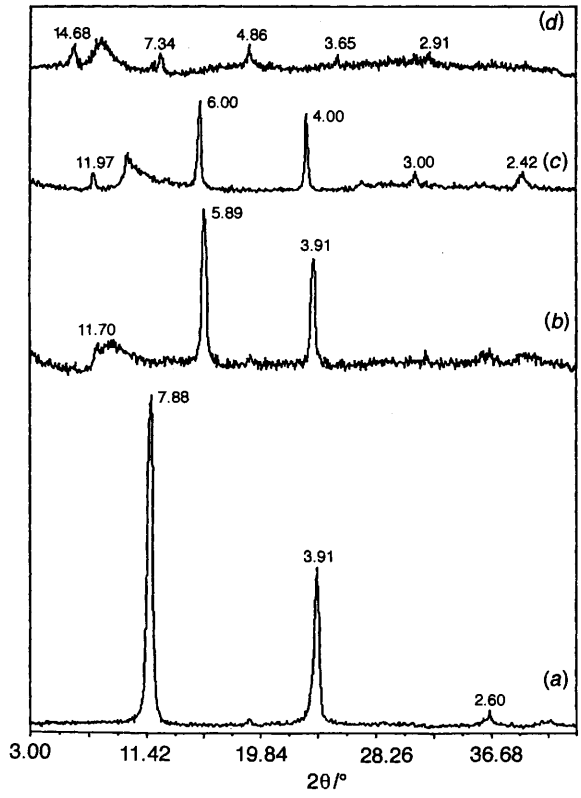

Fig. 1 X-Ray powder-diffraction patterns for oriented film samples of layered double hydroxide intercalates $MgAl[Cl^-]$ (*a*), $MgAl[V_{10}O_{28}^{6-}]$ (*b*), $MgAl[V_2W_4O_{19}^{4-}]$ (*c*) and $MgAl[Ti_2W_{10}PO_{40}^{7-}]$ (*d*). Values adjacent to the diffraction peaks are *d* spacings in Å for several 00*l* harmonics

with the basic MgAl layered double hydroxide. The ion $[Nb_2W_4O_{19}]^{4-}$, on the other hand, is stable in the range 4.5 < pH < 7.5 and is better matched with the more acidic ZnAl layered double hydroxide. Only in the case of the vanadates and vanadotungstates, acid addition was required in order to maintain the pH at mildly acidic values.

Powder X-ray diffraction. Good quality XRD diagrams were obtained which showed the absence of reflections due to the starting material and the appearance of several new equally spaced (00*l*) harmonics (and a broad, asymmetric peak at 2θ 7–11° the origin of which will be discussed below) with the (003) reflection having shifted to lower 2θ angles (Fig. 1). Well ordered basal spacings of about 12 Å were observed for the hexametalate-anion-pillared layered double hydroxides (Table 1) and a typical XRD pattern is shown for $MgAl[V_2W_4O_{19}^{4-}]$ [Fig. 1(*c*)]. Subtracting 4.8 Å for the thickness of a brucite layer gives a gallery height of 7.2 Å which is consistent with a monolayer of octahedral $M_6O_{19}^{n-}$ ions oriented with their C_3 axes (shortest dimension) perpendicular to the host layers. The structurally related decavanadate ion adopts an equivalent orientation with its C_2 axis parallel to the layers. Both configurations optimise hydrogen-bonding interactions with the hydroxide frameworks and afford products with the lowest free energy.[7] The shortest van der Waals diameter for ions of the type α-$XM_{12}O_{40}^{n-}$ is 9.9 Å along the C_2 axis and a basal spacing of *ca.* 14.7 Å is therefore predicted.[6] This is indeed what is observed for the $[HV_4W_8PO_{40}]^{6-}$ and $[Ti_2W_{10}PO_{40}]^{7-}$ layered double hydroxide intercalates, in agreement with other reported Keggin-ion intercalates.[6]

The Preyssler[23] anion, $[NaP_5W_{30}O_{110}]^{14-}$, is one of the largest known polyanions and is a rare example of a chemical assembly with a true five-fold symmetry axis (Fig. 2).[24] It is hydrolytically stable at room temperature at pH 0–11 and this makes it an attractive layered double hydroxide pillaring agent.

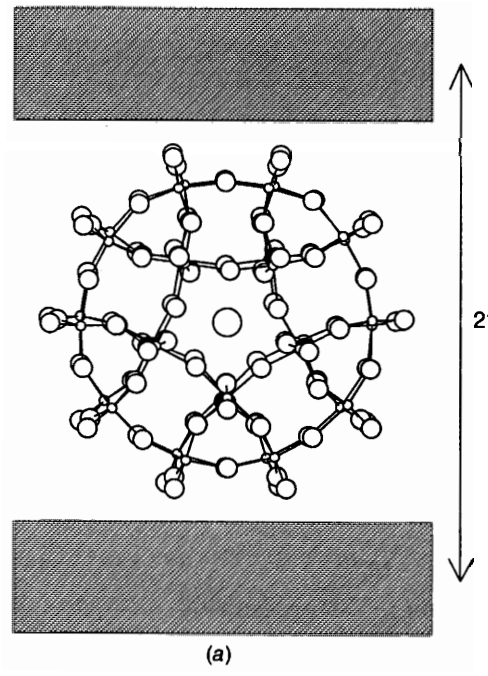

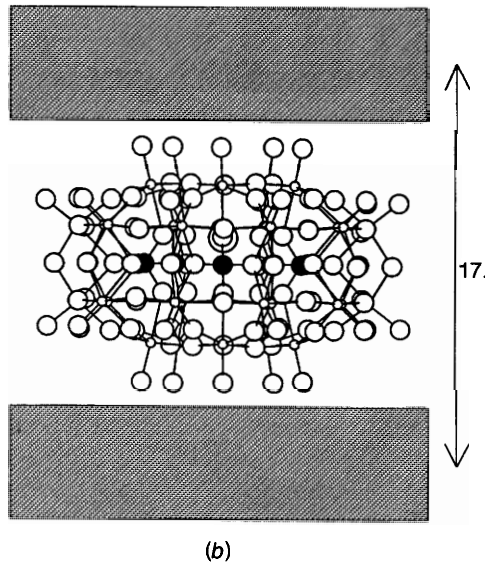

Fig. 2 Representation of $[NaP_5W_{30}O_{110}]^{14-}$ incorporated into a layered double hydroxide host with its C_5 axis parallel (*a*) and perpendicular (*b*) to the brucite-like layers. Interlayer spacings have been calculated given that the long and short dimensions of the cluster ion are 17.0 and 12.2 Å respectively (van der Waals radius of oxygen 1.4 Å). The thickness of a double hydroxide layer is taken to be 4.8 Å. Small open circles represent tungsten, medium open circles oxygen, medium filled circles phosphorus and the large open circle the sodium atom. Atomic coordinates from ref. 24

The structure consists of a cyclic arrangement of five PW_6O_{22} units, each formally derived from the Keggin-type ion $[PW_{12}O_{40}]^{3-}$ by removal of two sets of corner-shared WO_6 groups. The sodium atom is located on the five-fold axis at the centre of one of the two 10-membered rings of WO_6 octahedra. The ion appears as a prolate spheroid and there are two extreme orientations that it could adopt within the interlayer of a double hydroxide (Fig. 2). With the C_5 axis parallel to the layers and the ions in a rectangular arrangement the area per unit charge on the interlayer is 14.8 Å^2. With the C_5 axis perpendicular to the layers and the ions in a triangular arrangement the area per unit charge on the interlayer is 17.9 Å^2. In both of these orientations the ions should be spatially capable of balancing the host layer

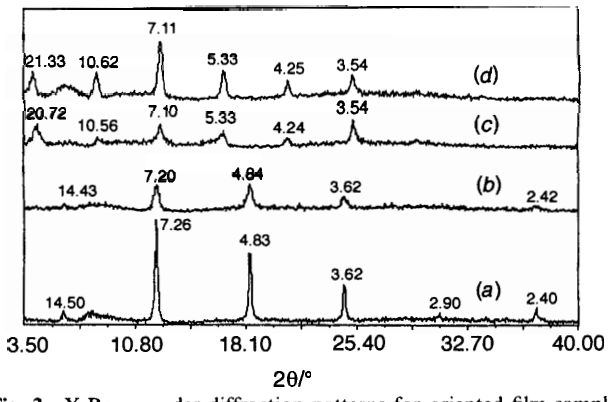

Fig. 3 X-Ray powder-diffraction patterns for oriented film samples of layered double hydroxide intercalates $ZnAl[Ti_2W_{10}PO_{40}^{7-}]$, prepared *via* $ZnAl[NO_3^-]$ (*a*) and by direct synthesis (*b*), and $ZnAl[NaP_5W_{30}O_{110}^{14-}]$, prepared *via* $ZnAl[NO_3^-]$ (*c*) and by direct synthesis (*d*). Values adjacent to the diffraction peaks are *d* spacings in Å for several 00*l* harmonics

charge of a layered double hydroxide with $Zn^{II}:Al^{III} = 1.3:1$, although the ions would be packed uncomfortably close in the second configuration (the area per unit layer charge is 19.2 Å^2 with this EDX-determined cation ratio). Seven (00*l*) reflections are observed between 2θ values of 3 and 40° in the preferred orientation XRD (POXRD) pattern of $ZnAl[NaP_5W_{30}O_{110}^{14-}]$ obtained *via* $ZnAl[NO_3^-]$ [Fig. 3(*c*)], assignable to a pillared phase with a basal spacing of 21 Å. Therefore, the ion orients itself with its shortest dimension parallel to the host layers.

Most of the XRD patterns obtained in this work contain a broad reflection at low angle (2θ 7–11°) which has been attributed in the literature to either a quasi-crystalline M^{II}/M^{III} salt of the polyoxometalate[12] or a disordered layered phase resulting from the cluster ions fitting into defects in the brucite-like layers.[6] Both theories indicate that pH is important, *i.e.* that formation of the polyoxometalate layered double hydroxide under acidic conditions could result in partial dissolution of cations from the hydroxide framework resulting in formation of a mixed salt and/or removal of hydroxide groups from the layers. However, the present results conflict with these ideas in that materials with similar X-ray tracings have been prepared over a wide pH range, from mildly acidic in the case of the vanadium-containing ions to mildly basic in the case of the niobotungstates. Furthermore, a $MgAl[V_2W_4O_{19}^{4-}]$ layered double hydroxide was successfully prepared in dichloromethane–ethanol and displayed an identical diffraction pattern to that obtained for the same material prepared by the more conventional aqueous method [Fig. 1(*c*)], albeit for some unexchanged starting material. Further work is clearly required to characterise this phenomenon.

Infrared spectroscopy, surface-area measurements and EDX data. Infrared spectroscopy was applied to establish first the presence or absence of carbonate in the clays (ν_3 absorption band at 1370 cm^{-1}), secondly the extent of ion exchange (where precursor ion is NO_3^-, ν_3 absorption band at 1384 cm^{-1}) and thirdly confirmation of retention of the polyoxometalate structure in the intercalated state. In the spectra of all the polyoxometalate layered double hydroxides characteristic bands of the polyoxometalates appear in the range 1200–400 cm^{-1} on top of the lattice vibrations of the host (Table 2). Materials prepared with pH < 7 were free of carbonate whereas those prepared under more basic conditions suffered a small degree of interference (weak ν_3 absorption band at 1370 cm^{-1}). The absence of the ν_3 absorption band at 1384 cm^{-1} in the spectra of the products obtained from $ZnAl[NO_3^-]$ confirmed that complete conversion into the pillared phase had taken place.

Table 1 Representative reaction conditions and observed basal spacings (d_{003}) for polyoxometalate-anion-pillared layered double hydroxides prepared *via* chloride-, nitrate- or benzenecarboxylate-anion-pillared precursors

Sample	X[a]	n_p[b]/mmol	c_p[c]/mol dm^{-3}	pH	d_{003}/Å
MgAl[$V_{10}O_{28}^{6-}$]	Cl^-	1.3	0.025	4.5	11.70
MgAl[$V_2W_4O_{19}^{4-}$]	Cl^-	1.5	0.024	4.7–5.0	11.97
MgAl[$Nb_2W_4O_{19}^{4-}$]	Cl^-	1.7	0.025	5.8–9.8	12.07
MgAl[$Nb_3W_3O_{19}^{5-}$]	Cl^-	0.13	0.017	9.0–11.1	12.18
MgAl[$Nb_4W_2O_{19}^{6-}$]	Cl^-	1.5	0.022	10.5–11.6	12.47
MgAl[$Ti_2W_{10}PO_{40}^{7-}$]	Cl^-	0.99	0.014	6.2–10.2	14.68
MgAl[$HV_4W_8PO_{40}^{6-}$]	Cl^-	1.1	0.014	4.3–5.0	14.53
ZnAl[$Ti_2W_{10}PO_{40}^{7-}$]	NO_3^-	0.53	0.011	—	14.50
ZnAl[$NaP_5W_{30}O_{110}^{14-}$]	NO_3^-	0.30	0.006	—	20.72
ZnCr[$V_{10}O_{28}^{6-}$]	4-$^-O_2CC_6H_4CO_2^-$	1.3	0.047	4.5	11.82
NiAl[$V_2W_4O_{19}^{4-}$]	4-$MeC_6H_4CO_2^-$	0.24	0.008	4.6	11.90
ZnAl[$SiW_{12}O_{40}^{4-}$]	4-$HOC_6H_4CO_2^-$	0.074	0.022	3.4–3.8	14.55
ZnAl[$BW_{12}O_{40}^{5-}$]	4-$HOC_6H_4CO_2^-$	0.55	0.017	3.8–4.0	14.57
ZnAl[$V_2W_{10}PO_{40}^{5-}$]	4-$MeC_6H_4CO_2^-$	0.57	0.018	3.6	14.71
ZnAl[$HV_4W_8PO_{40}^{6-}$]	4-$MeC_6H_4CO_2^-$	0.50	0.016	3.2–3.5	14.40

[a] X is the exchanging anion in the precursor. [b] Number of moles of polyoxometalate treated with precursor slurry containing 1.0 g clay material. [c] Polyoxometalate concentration.

Table 2 Characteristic IR bands in the region 2000–400 cm^{-1} for layered double hydroxide intercalates obtained by ion exchange

Sample	$\tilde{\nu}_{max}$*/cm^{-1}
MgAl[$V_{10}O_{28}^{6-}$]	1625m, 1403vw, 962s, 817m, 736m, 671m, 554w, 447vs
MgAl[$V_2W_4O_{19}^{4-}$]	1619m, 957s, 774s, 667m, 446vs
MgAl[$Nb_2W_4O_{19}^{4-}$]	1626m, 1369w, 1022vw, 961m, 897m, 770s (br), 669m, 568m, 445vs
MgAl[$Nb_3W_3O_{19}^{5-}$]	1626m, 1366m, 1022vw, 946w, 870w, 768s (br), 668 (sh), 559 (sh), 448vs
MgAl[$Nb_4W_2O_{19}^{6-}$]	1634m, 1366m, 1100vw, 1024vw, 935w, 844w, 769s (br), 669m, 556m, 448vs
MgAl[$Ti_2W_{10}PO_{40}^{7-}$]	1625m, 1366m, 1083m, 1063m, 1045m, 961s, 883w, 802vs (br), 668w, 555w, 448vs
MgAl[$HV_4W_8PO_{40}^{6-}$]	1625m, 1401w, 1099m, 1074m, 1052m, 970s, 880m, 780vs, 669s, 600w, 560m, 498m, 447s
ZnAl[$Ti_2W_{10}PO_{40}^{7-}$]	1622m, 1083m, 1063m, 1047m, 958s, 883w, 793vs (br), 618s, 594vw, 516vw, 483w, 428s
ZnAl[$NaP_5W_{30}O_{110}^{14-}$]	1615m, 1164m, 1081w, 1019w, 984vw, 938s, 913w, 789s, 730w, 619w, 571vw, 545vw, 426s
NiAl[$V_2W_4O_{19}^{4-}$]	1615m, 1539m, 1402m, 956s, 775vs, 624m, 570m, 432vs
ZnAl[$SiW_{12}O_{40}^{4-}$]	1623m, 1385w, 1096 (sh), 1006m, 951s, 925vs, 791vs, 721s, 619m, 543w
ZnAl[$BW_{12}O_{40}^{5-}$]	1613m, 1542m, 1441m, 1404m, 1013m, 961s, 922s, 823vs, 624m, 549m
ZnAl[$V_2W_{10}PO_{40}^{5-}$]	1603m, 1555m, 1440s, 1252m, 968s, 884m, 795vs, 620m, 423m
ZnAl[$HV_4W_8PO_{40}^{6-}$]	1614m, 1532m, 1405m, 1099m, 1076m, 1055m, 964s, 882s, 770vs, 626s, 558m, 426vs

* v = Very, s = strong, m = medium, w = weak, br = broad.

The BET (N_2) surface areas were in the range 22–32 m^2 g^{-1} for the MgAl intercalates which represent only a slight increase over those measured for the starting materials. For example, MgAl[$HV_4W_8PO_{40}^{6-}$] exhibited a surface area of 22 m^2 g^{-1} compared with 17 m^2 g^{-1} for the MgAl[Cl^-] precursor. Drezdon[7] found similar values for the similarly dried intercalates MgAl[$V_{10}O_{28}^{6-}$] and MgAl[$Mo_7O_{24}^{6-}$] prepared *via* a terephthalate-anion-pillared precursor. It was concluded that these areas were consistent with a model that approximated the clay samples as a close-packed array of non-porous spheres 1000–2000 Å in diameter (assuming that the space remaining in the interlayer region of the pillared hydrotalcites is filled with water).

The EDX-determined mole fractions of aluminium were between 0.37 and 0.35 for MgAl (except 0.40 for decavanadate-anion-pillared material) and 0.43 for ZnAl layered double hydroxides (Table 3). Given these aluminium contents, the EDX-determined polyoxoanion loadings are at least 75% of the theoretical maximum.

EXAFS studies. In the preceding paper we have shown that the EXAFS spectra for a series of structurally diverse polyoxometalates are rich in detail about the metal–oxygen bonds and also the non-bonded metal–metal relationships which define the cluster geometries.[22] Curve-fitting analysis enables an element-specific and sometimes complete characterisation of each anion. These studies have thus been extended to further verify that the structures of polyoxometalates are retained when incorporated into the galleries of layered double hydroxides (Table 4). This is exemplified by comparing the niobium K-edge EXAFS and Fourier transforms obtained for [$Nb_4W_2O_{19}$]$^{6-}$, as a pure salt and in the intercalated state (Fig. 4). The best fits to the EXAFS of the hexametalate anions were generally obtained with one OM terminal oxygen at 1.72–1.76 Å, four OM_2 doubly bridged oxygens at 1.88–1.99 Å, four metals at 3.20–3.34 Å and one metal atom at 4.74–4.78 Å. The tungsten L_{III}-edge EXAFS of [$Ti_2W_{10}PO_{40}$]$^{7-}$ and [$HV_4W_8PO_{40}$]$^{6-}$ were fitted by five-shell models comprising one OW terminal oxygen at 1.70–1.72 Å, four OW_2 doubly bridged oxygens at 1.88–1.89 Å, one tungsten at 3.39–3.41 Å, 1.5–1.6 tungstens at 3.68–3.70 Å and one vanadium or titanium atom at 3.32–3.35 Å. In all cases the EXAFS results strongly confirmed retention of the polyoxometalate structure.

Direct synthesis of polyoxometalate layered double hydroxides

Pillared derivatives ZnAl[$Ti_2W_{10}PO_{40}^{7-}$], ZnAl[$NaP_5W_{30}O_{110}^{14-}$] and MgAl[$Nb_4W_2O_{19}^{6-}$] were prepared by direct coprecipitation at pH 7.6, 8.4 and 9.6 respectively. Nitrate interference was small (weak ν_3 absorption band at 1384 cm^{-1}), negligible (very weak ν_3) and significant (strong ν_3) respectively. This method affords a very quick route to these materials but there must be pH compatibility between the host and guest species. Very good quality POXRD patterns were obtained for the ZnAl derivatives which compare well with their counterparts prepared *via* ZnAl[NO_3^-] (Fig. 3). The pattern for MgAl[$Nb_4W_2O_{19}^{6-}$] was of lower quality [broad and low intensity (00*l*) diffraction lines].

Synthesis of polyoxometalate layered double oxides *via* benzenecarboxylate-anion-pillared precursors

Layered double hydroxides of ZnAl, ZnCr and NiAl pillared by toluene-*p*-sulfonate and a series of benzenecarboxylate

Table 3 The EDX-determined metal atom ratios for polyoxometalate-anion-pillared layered double hydroxides prepared *via* chloride-, nitrate- or benzenecarboxylate-anion-pillared precursors[a]

Sample[b]	Mg	Al	Zn	W	Nb	V	Ti	L[c] (%)
$MgAl[V_{10}O_{28}^{6-}]$	1.49	1.00				1.28		77
$MgAl[V_2W_4O_{19}^{4-}]$	1.88	1.00		0.95		0.37		88
$MgAl[Nb_2W_4O_{19}^{4-}]$	1.70	1.00		0.83	0.49			88
$MgAl[Nb_3W_3O_{19}^{5-}]$	1.78	1.00		0.52	0.69			101
$MgAl[Nb_4W_2O_{19}^{6-}]$	1.72	1.00		0.40	0.80			121
$MgAl[Ti_2W_{10}PO_{40}^{7-}]$	1.89	1.00		1.23			0.24	84
$MgAl[HV_4W_8PO_{40}^{6-}]$	1.85	1.00		1.01		0.59		80
$ZnAl[Ti_2W_{10}PO_{40}^{7-}]$		1.00	1.29	1.91			0.37	131
$ZnAl[NaP_5W_{30}O_{110}^{14-}]$		1.00	1.30	3.77				176
$ZnAl[V_2W_{10}PO_{40}^{5-}]$		1.00	0.99	0.91		0.20		50
$ZnAl[HV_4W_8PO_{40}^{6-}]$		1.00	1.17	0.32		0.17		26

[a] Values accurate to 15%. [b] All of the products are detailed in Table 1. [c] Polyoxoanion loadings as a percentage of the theoretical maximum calculated from the EDX-determined mole fractions of aluminium.

Table 4 The EXAFS-derived structural parameters for polyxometalate salts and polyoxometalate-anion-pillared layered double hydroxides

					Polyoxometalate[b]				MgAl layered double hydroxides			
Anion	Edge	E_v[a]/eV	Shell	Co-ordination number	r[c]/Å	$2\sigma^2$[d]/Å^2	$E°$/eV	R (%)	r/Å	$2\sigma^2$/Å^2	$E°$/eV	R (%)
$[Nb_2W_4O_{19}]^{4-}$	W L_{III}	−8.0	O	1.0	1.716(6)	0.0051(10)	11.2	37.5	1.739(5)	0.0043(8)	11.6	37.5
			O	4.0	1.907(4)	0.0090(6)			1.904(4)	0.0099(6)		
			W	2.5	3.313(3)	0.0043(3)			3.309(3)	0.0061(3)		
			Nb	1.5	3.335(5)	0.0041(8)			3.333(5)	0.0062(9)		
	Nb K	−4.5	O	1.0	1.741(4)	0.0030(7)	25.6	31.2	1.746(7)	0.0070(13)	25.2	41.0
			O	4.0	1.994(3)	0.0077(5)			1.988(4)	0.0094(6)		
			W	2.8	3.320(2)	0.0049(3)			3.318(3)	0.0064(4)		
			Nb	1.2	3.350(5)	0.0039(9)			3.343(6)	0.0052(10)		
			W	1.0	4.737(5)	0.0039(9)			4.743(8)	0.0071(11)		
$[Nb_3W_3O_{19}]^{5-}$	W L_{III}	−7.5	O	1.0	1.743(5)	0.0042(7)	11.6	35.3	1.728(5)	0.0039(8)	11.5	35.7
			O	4.0	1.910(3)	0.0062(3)			1.900(3)	0.0063(3)		
			W	2.0	3.295(3)	0.0048(4)			3.301(3)	0.0037(4)		
			Nb	2.0	3.316(3)	0.0024(4)			3.320(3)	0.0016(4)		
			Nb	1.0	4.780(7)	0.0049(9)			4.771(6)	0.0039(9)		
	Nb K	−5.5	O	1.0	1.763(4)	0.0045(6)	24.3	30.2	1.760(4)	0.0052(8)	24.4	31.5
			O	4.0	1.988(2)	0.0082(4)			1.981(2)	0.0078(4)		
			W	2.0	3.327(2)	0.0059(2)			3.324(2)	0.0055(2)		
			Nb	2.0	3.337(3)	0.0090(5)			3.338(3)	0.0068(5)		
$[Nb_4W_2O_{19}]^{6-}$	W L_{III}	−7.0	O	1.0	1.720(4)	0.0014(5)	14.4	33.4	1.730(5)	0.0031(7)	12.7	36.9
			O	4.0	1.891(3)	0.0058(3)			1.895(3)	0.0067(4)		
			W	1.0	3.295(8)	0.0064(10)			3.313(11)	0.0082(14)		
			Nb	3.0	3.310(3)	0.0051(4)			3.316(4)	0.0064(4)		
			Nb	1.0	4.735(6)	0.0032(7)			4.754(6)	0.0035(8)		
	Nb K	−4.8	O	1.0	1.756(3)	0.0036(5)	25.8	25.3	1.759(3)	0.0039(6)	27.2	33.5
			O	4.0	1.979(2)	0.0085(3)			1.975(3)	0.0089(4)		
			W	1.5	3.338(2)	0.0052(2)			3.339(3)	0.0066(3)		
			Nb	2.5	3.329(2)	0.0083(3)			3.335(3)	0.0087(4)		
$[V_2W_4O_{19}]^{4-}$	W L_{III}	−7.0	O	1.0	1.743(6)	0.0049(9)	9.6	32.7	1.736(9)	0.0058(14)	9.3	41.2
			O	4.0	1.919(4)	0.0094(6)			1.915(5)	0.0099(7)		
			W	2.5	3.272(2)	0.0044(1)			3.278(3)	0.0053(2)		
			V	1.5	3.197(5)	0.0049(8)			3.206(7)	0.0050(11)		
$[Ti_2W_{10}PO_{40}]^{7-}$	W L_{III}	−5.0	O	1.0	1.707(4)	0.0048(6)	15.4	28.5	1.714(3)	0.0033(4)	14.2	23.0
			O	4.0	1.881(3)	0.0139(5)			1.881(3)	0.0133(4)		
			W	1.0	3.406(3)	0.0034(3)			3.413(2)	0.0059(3)		
			W	1.6	3.695(3)	0.0074(4)			3.697(4)	0.0099(6)		
			Ti	1.0	3.347(5)	0.0036(8)			3.350(4)	0.0043(8)		
$[HV_4W_8PO_{40}]^{6-}$	W L_{III}	−5.0	O	1.0	1.699(4)	0.0046(6)	13.4	32.1	1.718(4)	0.0044(6)	14.3	28.5
			O	4.0	1.883(3)	0.0122(4)			1.885(3)	0.0121(4)		
			W	1.0	3.392(3)	0.0048(4)			3.400(3)	0.0038(4)		
			W	1.5	3.684(5)	0.0112(9)			3.684(7)	0.0130(11)		
			V	1.0	3.321(4)	0.0031(7)			3.325(4)	0.0016(6)		

[a] Virtual potential representing inelastic losses and core-hole lifetime effects. [b] See Experimental section for counter ions. [c] Standard deviations in parentheses. [d] Debye–Waller factor; σ = root-mean-square internuclear separation.

anions were prepared using the direct coprecipitation method described by Drezdon[7] for the synthesis of similar MgAl derivatives. The XRD diagrams for each of the products contain up to five approximately equally spaced peaks which are readily assigned as the (00*l*) reflections of hydrotalcite-like phases with basal spacings between 14 and 18.4 Å [Table 5, Figs. 5(*a*) and 6(*a*)]. The values are in agreement with predictions based on a model in which the ions stack to form a monolayer with the aromatic rings perpendicular to the host layer (Table 5). Given that we have an ordered interlayer, the sharpness of the basal reflections is indicative of crystallite size in the *z* direction. This was found to be dependent on the nature of the layered double hydroxide cations, with the ZnAl clays consistently forming the best crystallised materials. This so-called particle-size-broadening effect is expressed quantitatively by the Scherrer equation,[25] $D = 0.9\lambda/(\beta_c \cos\theta)$, where D is the

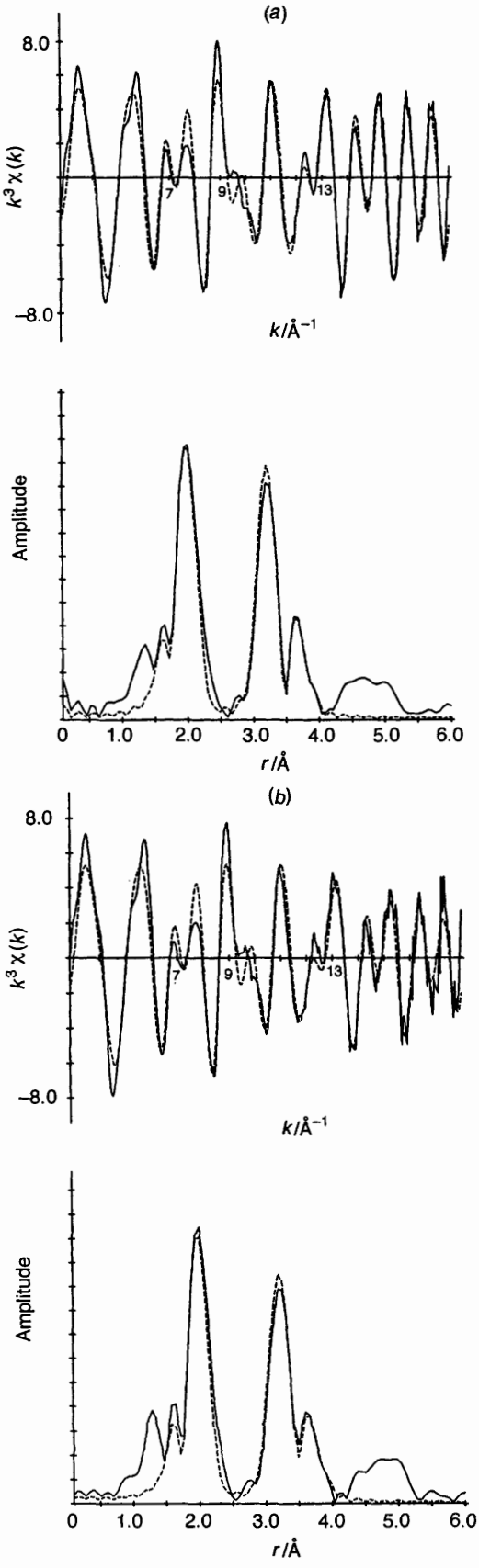

Fig. 4 Low-temperature (80 K) solid-state niobium K-edge k^3-weighted EXAFS data and Fourier transform, phase-shift corrected for oxygen (——, experimental; —, spherical wave theory), of $Na_4K_2[Nb_4W_2O_{19}]$ (*a*) and the layered double hydroxide intercalate $MgAl[Nb_4W_2O_{19}^{6-}]$ (*b*)

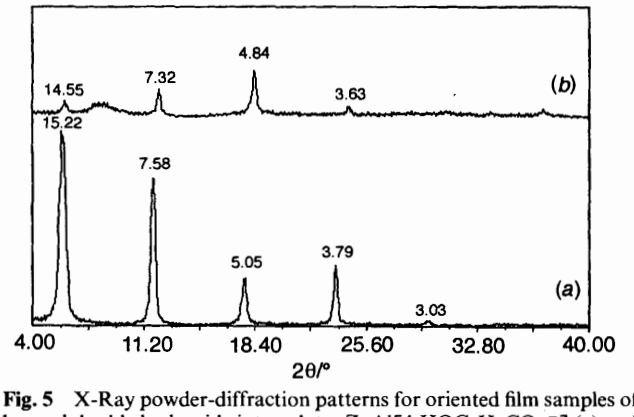

Fig. 5 X-Ray powder-diffraction patterns for oriented film samples of layered double hydroxide intercalates $ZnAl[4\text{-}HOC_6H_4CO_2^-]$ (*a*) and $ZnAl[\alpha\text{-}SiW_{12}O_{40}^{4-}]$ (*b*). Values adjacent to the diffraction peaks are *d* spacings in Å for several 00*l* harmonics

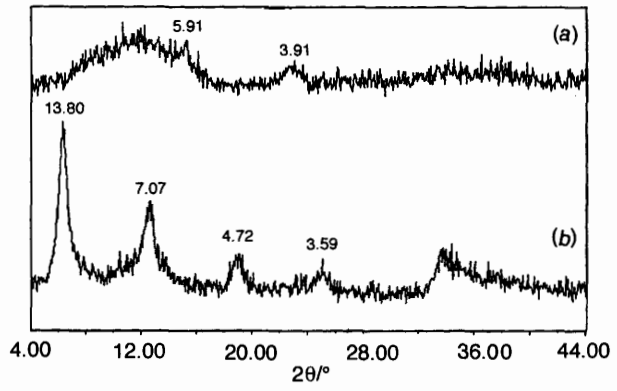

Fig. 6 X-Ray powder-diffraction patterns for oriented film samples of layered double hydroxide intercalates $ZnCr[4\text{-}^-O_2CC_6H_4CO_2^-]$ (*a*) and $ZnCr[V_{10}O_{28}^{6-}]$ (*b*). Values adjacent to the diffraction peaks are *d* spacings in Å for several 00*l* harmonics

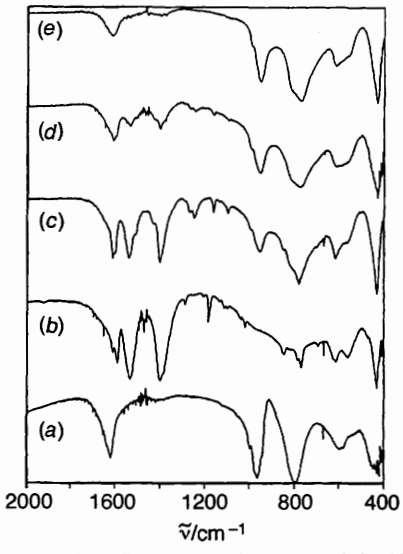

Fig. 7 Fourier-transform IR spectra of the layered double hydroxide intercalates obtained after ion exchange of $Na_4[V_2W_4O_{19}]$ (*a*) with $ZnAl[4\text{-}HOC_6H_4CO_2^-]$ (*b*) for 1 h at 25–35 (*c*), 50–60 (*d*) and 90–100 °C (*e*)

mean crystallite size (Å) along a line normal to the reflecting plane, λ the X-ray wavelength (1.5406 Å), β_c the instrument-corrected width of the (003) harmonic at half-height expressed in radians of 2θ, and θ is the diffraction angle. Values of *D* were mostly in the range 200–300 Å for the ZnAl in contrast to 100–120 Å for the NiAl and ZnCr layered double hydroxides.

Infrared spectroscopy showed that all of the products contained the carboxylate [ν_{max}/cm^{-1} 1550–1650s (CO_{asym}) and *ca.* 1400s (CO_{sym})] or sulfonate groups rather than the

Table 5 Reaction conditions and X-ray powder-diffraction data for organic-anion-pillared layered double hydroxides prepared by coprecipitation

Sample	T/°C	t/h	pH	2θ/° for (00l) harmonics					Basal spacing/Å		
				003	006	009	00, 12	00, 15	d_{obs}	$d_{calc.}$[a]	D[b]/Å
ZnAl[4-$HOC_6H_4CO_2^-$]	75	48	7.6	5.80	11.67	17.55	23.45	29.46	15.22	14.7	184
ZnAl[4-$MeC_6H_4CO_2^-$]	74	48	7.5	5.12	10.37	15.45	20.79	26.11	17.25	17.7	263
ZnAl[4-$O_2CC_6H_4CO_2^-$]	75	48	7.7	6.24	12.46	18.83	25.28	—	14.15	14.62	255
ZnAl[4-$O_2NC_6H_4CO_2^-$]	71	48	7.7	6.16	12.32	18.55	22.49	—	14.33	14.57	247
ZnAl[4-$EtC_6H_4CO_2^-$]	74	96	7.7	4.98	9.96	15.03	20.03	24.99	17.73	17.9	193
ZnAl[4-$^-O_2CC_6H_4C_6H_4CO_2^-$-4]	71	48	7.7	4.80	9.66	14.39	19.32	24.17	18.39	18.96	226
ZnAl[4-$MeC_6H_4SO_3^-$]	66	48	8.0	5.28	10.60	15.70	20.93	26.11	16.72	17.5	394
ZnAl[pipes]	67	48	7.6	6.02	12.11	18.32	24.43	—	14.67	22.58	343
NiAl[4-$^-O_2CC_6H_4CO_2^-$]	68	18	8.0	6.16	12.27	18.61	24.68	—	14.33	14.62	94
ZnCr[4-$^-O_2CC_6H_4CO_2^-$]	65	18	7.9	6.40	12.51	18.77	24.80	—	13.80	14.62	118
CuAl[4-$MeC_6H_4CO_2^-$]	60	18	8.0	5.18	10.33	15.52	20.70	25.99	17.04	17.7	198
NiAl[4-$MeC_6H_4CO_2^-$]	75	96	7.8	5.20	10.40	15.48	20.81	26.01	16.98	17.7	117

[a] Assumptions: monolayer with aromatic or heterocyclic rings oriented perpendicular to the brucite-like layers; van der Waals radii of oxygen 1.4 Å and of hydrogen 1.2 Å. [b] Mean crystallite dimension along a line normal to the 00l reflecting planes [calculated from the (003) harmonic].

corresponding acids [Fig. 7(*b*)]. Thus, none of the spectra contained a peak at 1700–1750 cm^{-1} characteristic of the carboxylic acid dimer or monomer ($C{=}O_{asym}$). The EDX-determined $M^{II}:M^{III}$ ratios were 1.40:1 for ZnAl[4-$^-O_2CC_6H_4CO_2^-$], 2.01:1 for NiAl[4-$^-O_2CC_6H_4CO_2^-$], 2.02:1 for ZnCr[4-$^-O_2CC_6H_4CO_2^-$], 1.99:1 for ZnAl[4-$MeC_6H_4CO_2^-$], 1.87:1 for NiAl[4-$MeC_6H_4CO_2^-$], 1.70:1 for ZnAl[4-$HOC_6H_4CO_2^-$] and 3.50:1 for CuAl[4-$MeC_6H_4CO_2^-$]. A ZnAl layered double hydroxide pillared by the piperazine-1,4-bis(ethanesulfonate) (pipes) dianion was also prepared. This gave an XRD diagram with narrow (00l) reflections but the observed layer spacing of 14.67 Å is considerably smaller than that expected with the piperazine ring lying perpendicular to the layers (22.6 Å). It follows that the molecule may be tilted at an angle of 34° to the layers.

Layered double hydroxides containing the ions $YC_6H_4CO_2^-$ (Y = CO_2^-, OH or Me) were investigated for their suitability as precursors to polyoxometalate derivatives. Ion exchange can only be facilitated under mildly acidic conditions (pH 3.5–4.5) when protonation of the carboxylate group(s) promotes migration of the molecule out of the interlayer. This process is inhibited by the poor solubility of the acids in water and the resulting difficulty in their removal from the clay matrix. In the case of terephthalate-anion-pillared precursors, the products had to be treated with hot methanol followed by hot water in order fully to extract the acid. 4-Hydroxybenzoic acid can however be washed out relatively easily with hot water. The ease and extent of ion exchange was found to improve in the order terephthalate < 4-methylbenzoate < 4-hydroxybenzoate. One advantage of this method is that both the precursor clay complexes and final products suffer negligible carbonate interference, even if strictly carbonate-free conditions are not employed.

Ion exchange in the ZnAl[4-$HOC_6H_4CO_2^-$]–[$V_2W_4O_{19}^{4-}$] system was complete within 1 h at 90–100 °C, as shown by a series of IR spectra taken as a function of reaction temperature (Fig. 7). The XRD diagram for the final product was very similar to that obtained for the MgAl analogue prepared from MgAl[Cl^-] [Fig. 1(*c*)] and gave a basal spacing of 12.00 Å. Complete conversion was also possible in the ZnAl[4-$HOC_6H_4CO_2^-$]–[$SiW_{12}O_{40}^{4-}$] (Fig. 5) and ZnAl[4-$HOC_6H_4CO_2^-$]–ZnAl[$BW_{12}O_{40}^{5-}$] systems. Keggin-type anions with charge −3 should be spatially incapable of balancing the host layer charge of a layered double hydroxide with $M^{II}:M^{III}$ = 2:1 (assuming each cluster ion occupies an area of 83 $Å^2$).[5,6] It was indeed found that no ion exchange took place in the ZnAl[4-$HOC_6H_4CO_2^-$]–[$PW_{12}O_{40}^{3-}$] system. Ion exchange was about 80% in the NiAl[4-$MeC_6H_4CO_2^-$]–[$V_2W_4O_{19}^{4-}$] and ZnAl[4-$MeC_6H_4CO_2^-$]–[$V_2W_4O_{19}^{4-}$] systems as evidenced by the weak carbonyl absorptions of the carboxylate group [ν_{max}/cm^{-1} 1589w (CO_{asym}) and 1401w (CO_{sym})]. The XRD diagrams of NiAl[$V_2W_4O_{19}^{4-}$] and ZnCr[$V_{10}O_{28}^{6-}$] were similar and did not contain any peaks due to the starting material [Fig. 6(*b*)].

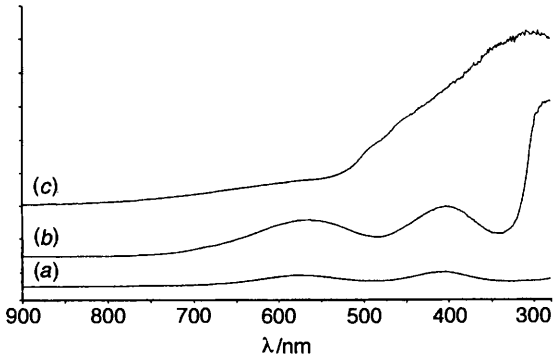

Fig. 8 UV/VIS spectra of an aqueous solution of $Cr_2(SO_4)_3$ (*a*), and diffuse reflectance spectra of the layered double hydroxide intercalates ZnCr[4-$^-O_2CC_6H_4CO_2^-$] (*b*) and ZnCr[$V_{10}O_{28}^{6-}$] (*c*)

UV/VIS spectroscopy. Diffuse-reflectance UV/VIS spectra were obtained for the ZnCr (Fig. 8) and NiAl systems. The three spin-allowed d–d transitions for a d^3 chromium(III) centre in an octahedral crystal field are $\nu_1 = {}^4T_{2g}(F) \longleftarrow {}^4A_{2g}(F)$ (= $10Dq$), $\nu_2 = {}^4T_{1g}(F) \longleftarrow {}^4A_{2g}(F)$ and $\nu_3 = {}^4T_{1g}(P) \longleftarrow {}^4A_{2g}(F)$.[26a] Two broad maxima are observed at ν_1 17 793 (562) and ν_2 25 000 cm^{-1} (400 nm) in the spectrum of violet ZnCr[4-$^-O_2CC_6H_4CO_2^-$] [Fig. 8(*b*)]; the third transition is obscured. Inputting the observed ν_1 and ν_2 into the equations published by Dou[27] for an A_2 ground-state ion yields Racah parameter B = 724 cm^{-1} and ν_3 39 236 cm^{-1} (255 nm). The value of B is in agreement with that found for $K[Cr(H_2O)_6][SO_4]_2{\cdot}6H_2O$ (725 cm^{-1}).[26a] In the spectrum of olive ZnCr[$V_{10}O_{28}^{6-}$] the ν_1 absorption is just visible as a weak shoulder but the ν_2 band is completely obscured by the strong absorption due to [$V_{10}O_{28}$]$^{6-}$ [Fig. 8(*c*)].

The three spin-allowed transitions for a d^8 nickel(II) centre in an octahedral field are $\nu_1 = {}^3T_{2g}(F) \longleftarrow {}^3A_{2g}(F)$ (= $10Dq$), $\nu_2 = {}^3T_{1g}(F) \longleftarrow {}^3A_{2g}(F)$ and $\nu_3 = {}^3T_{1g}(P) \longleftarrow {}^3A_{2g}(F)$.[26b] Maxima were observed at 376, 411 (shoulder), 650, 741 (shoulder) and 1102 nm (very broad) in the spectrum of pale green NiAl[4-$MeC_6H_4CO_2^-$]. Labajos *et al.*[28] obtained an identical spectrum for $Ni_2Al[CO_3^{2-}]$ but were limited to the wavelength range 250–850 nm. They assigned ν_2 13 495 (741) and ν_3 26 596 cm^{-1} (376 nm). In addition, the absorptions at 15 385 (650) and 24 331 cm^{-1} (411 nm) were attributed to the spin-forbidden transitions $\nu_4 = {}^1E_g(D) \longleftarrow {}^3A_{2g}(F)$ and ν_5 =

$^1T_{2g}(D) \longleftarrow {}^3A_{2g}(F)$ respectively which gain intensity due to spin–orbit coupling ['mixing' of the $^1E_g(D)$ and $^1T_{2g}(D)$ terms with the $^3T_{1g}(F)$ and $^3T_{1g}(P)$ terms respectively]. This assignment must however be treated with caution since there is poor agreement between the observed (9074 cm^{-1}) and calculated (7955 cm^{-1}, from ν_2 13 495 and ν_3 26 596 cm^{-1} using the equations of Dou)[27] values of ν_1. The spectrum of NiAl-$[V_2W_4O_{19}{}^{4-}]$ is identical to that of NiAl[4-$MeC_6H_4CO_2{}^-$] at wavelengths greater than 550 nm. Below this the broad intense absorption due to the tungstovanadate ion dominates (λ_{max} 395 nm).

EXAFS studies. The best fits to both the chromium K-edge EXAFS of ZnCr[4-$^-O_2CC_6H_4CO_2{}^-$] and ZnCr[$V_{10}O_{28}{}^{6-}$] were achieved with six oxygen atoms at 1.98 Å and six zinc atoms at 3.11 Å (Fig. 9, Table 6). The zinc shell is in accordance with Lowenstein's rule which states that (in aluminosilicates) trivalent cations should not be in adjacent metal sites.[29] This gives rise to an idealised model in which the cations are ordered so as to give a hexagonal supercell with dimension $a = a'\sqrt{3}$ where a' is the separation of adjacent cations (Fig. 10).[30] Consistent with this model, the zinc K-edge EXAFS of both layered double hydroxides were fitted by four-shell models comprising six oxygens at 2.06–2.07 Å, three zinc at 3.09 Å, three chromium at 3.11 Å and six zinc atoms at 5.36–5.37 Å (Fig. 11, Table 6). The similarity in the backscattering properties of chromium and zinc caused unacceptably high correlations between the structural parameters of the metal shells at 3.1 Å when they were refined together. Therefore the parameters for the chromium shell have been fixed at the values determined from the chromium K-edge data. A map of the EXAFS fit indices for the non-bonded Zn · · · Zn distance *versus* the non-bonded Zn · · · Cr distance for ZnCr[4-$^-O_2CC_6H_4CO_2{}^-$] supports this result as the point corresponding to Zn · · · Cr 3.11 Å and Zn · · · Zn 3.09 Å lies within an elongated minimum stretching between 3.11 and 3.16 Å for the Zn · · · Cr distance and between 3.09 and 3.07 Å for the Zn · · · Zn distance.

The Zn · · · Zn distance of 5.36–5.37 Å is in very good agreement with the expected value of 3.1 × $\sqrt{3}$ (5.37 Å). Furthermore, it is identical to the XRD-derived value of a_0 reported by Boehm *et al.*[31] for synthetic layered double hydroxides of the type $Zn_2Cr[X^{n-}]$ where X^{n-} = Cl^-, $NO_3{}^-$ or $SO_4{}^{2-}$. A Zn · · · M shell comprising three chromium and three zinc atoms is also expected at *ca.* 6.2 Å and indeed the Fourier transforms of the zinc K-edge EXAFS contain an intense peak at this distance. Attempts to solve this shell were however hampered by the fact that statistically valid shells could be fitted at both 6.01–6.06 and 6.33–6.39 Å (zinc and chromium interchangeable). For example, a final six-shell fit with R factor = 28.8% was obtained with three zinc atoms at 6.01 Å ($2\sigma^2$ 0.002 $Å^2$) and three chromium atoms at 6.39 Å ($2\sigma^2$ 0.001 $Å^2$).

The best fits to the nickel K-edge EXAFS of NiAl[4-$MeC_6H_4CO_2{}^-$] and NiAl[$V_2W_4O_{19}{}^{4-}$] were achieved with six oxygen at 2.04–2.05 Å, three nickel at 3.04 Å and six nickel atoms at 5.21 Å (Table 6). No acceptable fits were obtained with either an aluminium shell at about 3.0 Å or metal shells at about 6.2 Å. From the non-bonded Ni · · · Ni distance of 5.21 Å the separation of adjacent cations should be 3.01 Å. This is slightly shorter than that found but does agree very well with predictions based on the approximately linear relationship between values of the mole fraction of aluminium (x) and a_0 for layered double hydroxides of the type $Ni_{1-x}Al_x[X^{n-}]$.[32] The EXAFS results for both the NiAl and ZnCr systems indicate that no significant disruption of the layer structures took place during intercalative ion exchange of the cluster ions.

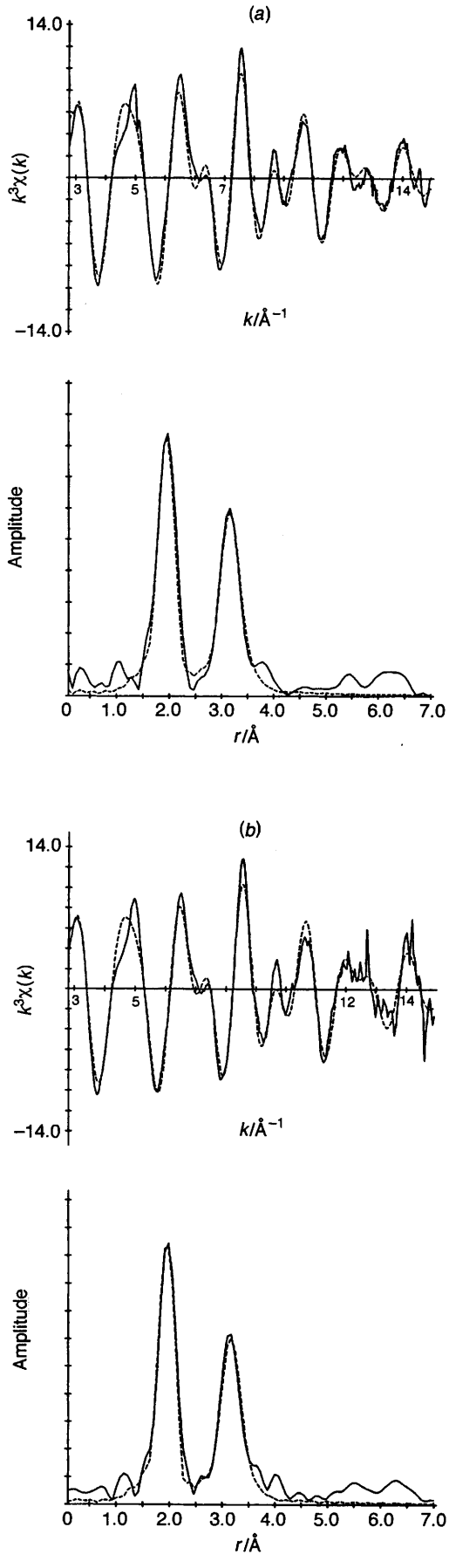

Fig. 9 Chromium K-edge k^3-weighted EXAFS data and Fourier transform of the layered double hydroxide intercalates ZnCr[4-$^-O_2CC_6H_4CO_2{}^-$] (*a*) and ZnCr[$V_{10}O_{28}{}^{6-}$] (*b*) in the solid state at 80 K. Details as in Fig. 4

Conclusion

Three of the more effective methods for the synthesis of polyoxometalate-anion-pillared layered double hydroxides

Table 6 The EXAFS-derived structural parameters for benzenecarboxylate- and polyoxometalate-anion-pillared layered double hydroxides

Product	Edge	Shell	Co-ordination number	r/Å	$2\sigma^2$/Å^2	$E°$/eV	R (%)
ZnCr[4-$^-O_2CC_6H_4CO_2^-$]	Cr K	O	6.0	1.977(2)	0.0075(3)	2.9	24.1
		Zn	6.0	3.110(2)	0.0142(3)		
	Zn K	O	6.0	2.062(4)	0.0150(9)	−2.3	36.9
		Zn	3.0	3.089(3)	0.0083(4)		
		Cr	3.0	3.110	0.014		
		Zn	6.0	5.364(8)	0.0115(13)		
ZnCr[$V_{10}O_{28}^{6-}$]	Cr K	O	6.0	1.973(2)	0.0056(3)	3.0	27.1
		Zn	6.0	3.107(3)	0.0139(4)		
	Zn K	O	6.0	2.070(4)	0.0106(8)	−2.2	38.3
		Zn	3.0	3.089(3)	0.0061(4)		
		Cr	3.0	3.110	0.014		
		Zn	6.0	5.371(8)	0.0108(15)		
NiAl[4-$MeC_6H_4CO_2^-$]	Ni K	O	6.0	2.045(3)	0.0080(5)	0.7	30.0
		Ni	3.0	3.038(3)	0.0100(6)		
		Ni	6.0	5.212(9)	0.0134(16)		
NiAl[$V_2W_4O_{19}^{4-}$]	Ni K	O	6.0	2.043(3)	0.0078(5)	0.9	32.1
		Ni	3.0	3.040(4)	0.0099(6)		
		Ni	6.0	5.213(9)	0.0132(16)		

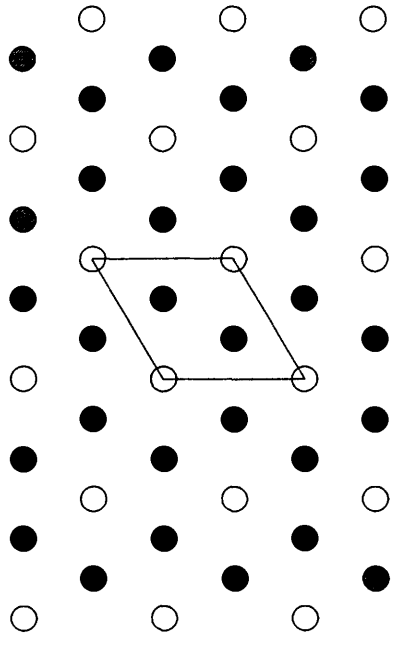

Fig. 10 Hexagonal supercell resulting from cation ordering in a layered double hydroxide with $M^{II}:M^{III} = 2:1$. Shaded circles represent M^{2+} ions and open circles M^{3+} ions

have been used to isolate new examples with gallery heights ranging from 7.1 to 16 Å. Ion exchange of chloride- or nitrate-ion-containing precursors is the more consistent approach in terms of high percentage conversion and product crystallinity. The choice of polyanion is not limited to those hydrolytically stable at pH < 5 as is the case when starting from organic-anion-pillared layered double hydroxides, when 4-methylbenzoate was found to be the best precursor ion out of a series investigated. Direct synthesis is the third and least general method used in that it demands pH compatibility between the host and guest species. Nevertheless, success was had in preparing the intercalate ZnAl[$NaP_5W_{30}O_{110}^{14-}$], with a well ordered and exceptionally large layer spacing of 21 Å.

Physical techniques such as IR and Raman spectroscopy go some way in the characterisation of the pillaring anion in the intercalated state but are short on detailed information. We have shown that EXAFS spectroscopy allows the metallic environments of both the host lattice and guest species to be probed in detail up to a distance of 6 Å from the absorber. Zinc, chromium and nickel K-edge EXAFS studies complement those of X-ray powder diffraction and indicate no disruption in the layer structures of ZnCr[$V_{10}O_{28}^{6-}$] and NiAl[$V_2W_4O_{19}^{4-}$] prepared from ZnCr[4-$^-O_2CC_6H_4CO_2^-$] and NiAl[4-$MeC_6H_4CO_2^-$] respectively at pH 4.5. It appears therefore that the less crystalline by-product observed for these and other examples is not the result of mixed salt formation or the polyoxometalate fitting into defects created in the hydroxide layers. These theories are further in doubt given that we have found the presence of the phase to be largely independent of the synthetic method, reaction pH or even solvent. Further studies are required to characterise this phenomenon. The EXAFS analysis data for the metal centres of the guest species has given direct structural evidence for intercalation of the cluster ions intact.

Experimental

Commercial materials were of reagent grade or better and used without further purification. Infrared spectra were measured from KBr pellets on a Perkin-Elmer 1710 spectrometer, solid-state UV/VIS spectra from undiluted samples using the diffuse-reflectance attachment of a Perkin-Elmer Lambda 19 spectrometer. Powder X-ray diffraction patterns were obtained using a Siemens D5000 diffractometer with Cu-Kα_1 radiation. Samples were typically step-scanned in 0.02° 2θ steps with a counting time of 0.6 s per step. Clay specimens for preferred-orientation XRD were prepared by evaporating dilute aqueous clay slurries onto microscope slides. Semiquantitative EDX analysis data were obtained using a JEOL JSM64000 scanning electron microscope operating with a 20 keV electron energy and fitted with a Tracor Northern series II X-ray and image analyser. The BET (N_2) surface areas were determined at 77 K as described previously.[33] Powders were dried at 100 °C for 1 h and degassed overnight (0.04 Torr) prior to measurement.

X-Ray absorption spectra were acquired using the Synchrotron Radiation Source at the Daresbury Laboratory and analysed as described previously[22] using the personal computer resident program PAXAS[34] for background subtraction and EXCURVE[35] (version EXCURV 92) for curve-fitting analysis. Values of AFAC, the energy-independent parameter used to take account of reduction in the EXAFS amplitude due to multiple excitations, were 0.95, 0.90, 0.80, 0.85 and 0.75 for the Nb K-, W L_{III}-, Ni K-, Zn K- and Cr K-edge spectra respectively. The phase shifts for the Nb K- and W L_{III}-edge spectra were calculated using Xα atomic potentials for the ground and excited states, whereas those for the Ni K-, Zn K- and Cr K-edge spectra were calculated with Von Bart ground-

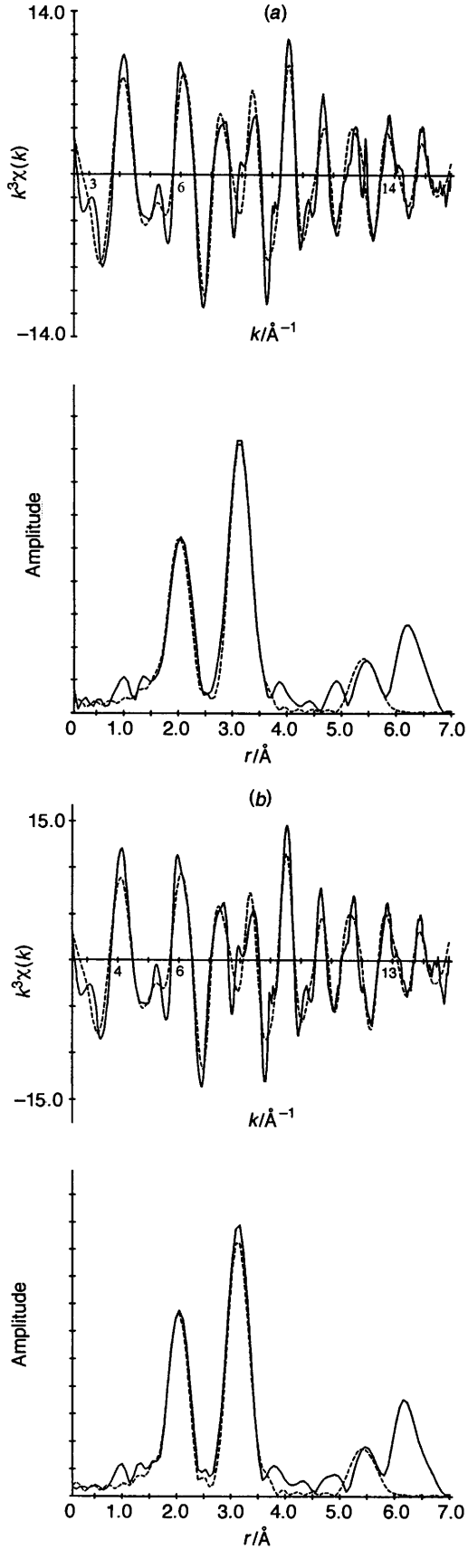

Fig. 11 Zinc K-edge k^3-weighted EXAFS data and Fourier transform of the layered double hydroxide intercalates ZnCr[4-$^-O_2CC_6H_4$-CO_2^-] (*a*) and ZnCr[$V_{10}O_{28}^{6-}$] (*b*) in the solid state at 80 K

state and Hedin Lundqvis exchange potentials. The EXAFS-derived structural information did not depend significantly on the type of potential used.

The following polyoxometalate salts were prepared and purified as reported previously: $K_7[HNb_6O_{19}]$,[36] $Na_4[V_2W_4O_{19}]$,[37] $[NMe_4][Na_2KNb_2W_4O_{19}]$,[38] $[NMe_4]Na_2K_2[Nb_3W_3O_{19}]$,[38] $Na_4K_2[Nb_4W_2O_{19}]$,[38] $[NH_4]_6[V_{10}O_{28}]$,[39] $K_4[SiW_{12}O_{40}]$,[40] $K_5[BW_{12}O_{40}]$,[41] $K_7[Ti_2W_{10}PO_{40}]$,[42] $K_5[V_2W_{10}PO_{40}]$,[43] $[NH_4]_6[HV_4W_8PO_{40}]$[44] and $K_{12.5}Na_{1.5}[NaP_5W_{30}O_{110}]$.[45] All samples were identified in the solid state by their IR spectra, which agreed with those found previously for the same compounds.[23,24,37,42,46] The niobate complexes $Nb_xW_{6-x}O_{19}^{(x+2)-}$ were further characterised in solution by their UV spectra.[38]

Synthesis of polyoxometalate-anion-pillared layered double hydroxides

Typical procedures are described below. Table 1 gives details of the products obtained *via* nitrate-, chloride- or benzenecarboxylate-anion-containing layered double hydroxides. Carbonate-free 50% NaOH stock solution was prepared by dissolving 99.99% semiconductor-grade NaOH pellets (Aldrich) in decarbonated deionised distilled water and stored under N_2. The final products were generally isolated by filtration or centrifugation, washed with methanol and/or decarbonated water and dried at room temperature under reduced pressure in a vacuum desiccator.

***via* MgAl[Cl^-], MgAl[NO_3^-] or ZnAl[NO_3^-].** The precursor materials were synthesised under nitrogen atmospheres using procedures similar to that described by Reichle and Meyn *et al.*[47]

(*a*) MgAl[Cl^-]. A solution of $MgCl_2{\cdot}6H_2O$ (25.82 g, 127 mmol) and $AlCl_3{\cdot}6H_2O$ (15.29 g, 63 mmol) in decarbonated water (130 cm^3) was added dropwise within 1 h to a vigorously stirred solution of 50% NaOH (31.2 g, 390 mmol) and NaCl (12.29 g, 210 mmol) in decarbonated water (130 cm^3). The final pH after addition was about 10. The precipitate was aged at 95 °C for 6 d, washed by centrifugation with decarbonated water and stored as an aqueous slurry in a sealed container. Net weight of clay in final slurry (320 cm^3) = 9.2 g (corresponding to material dried at room temperature under reduced pressure in a vacuum desiccator). The MgAl[NO_3^-] was prepared in exactly the same manner using $Mg(NO_3)_2{\cdot}6H_2O$, $Al(NO_3)_3{\cdot}9H_2O$ and $NaNO_3$ (precipitate aged at 95 °C for 7.5 d). Net weight of clay in final slurry (324 cm^3) = 12.3 g.

(*b*) ZnAl[NO_3^-]. A solution of $Zn(NO_3)_2{\cdot}6H_2O$ (6.84 g, 23 mmol) and $Al(NO_3)_3{\cdot}9H_2O$ (4.50 g, 12 mmol) in decarbonated water (60 cm^3) was added dropwise within 30 min to a vigorously stirred solution of 50% NaOH (5.6 g, 70 mmol) and $NaNO_3$ (3.4 g, 40 mmol) in decarbonated water (60 cm^3). The final pH after addition was about 7. The precipitate was aged at 85 °C for 18 h, cooled to ambient temperature, washed by filtration with decarbonated water and stored as an aqueous slurry in a sealed container. Net weight of clay in final slurry (100 cm^3) = 4.0 g.

(*c*) *Ion exchange.* Table 1 details the conditions for each aqueous ion-exchange reaction. A typical reaction scale was 50 cm^3 and involved dropwise addition with stirring of a solution of the polyoxometalate (up to 100% in excess over that theoretically required for complete exchange) to the clay slurry (MgAl) or *vice versa* (ZnAl layered double hydroxides). The MgAl mixtures were then stirred at room temperature for up to 1 h; ZnAl[$Ti_2W_{10}PO_{40}^{7-}$] was formed by reaction at 100 °C for 35 min, ZnAl[$NaP_5W_{30}O_{110}^{14-}$] reaction at 80 °C for 2 h. Only in the case of the vanadium-containing polyoxometalates the pH of the reaction mixture was controlled (4.0–5.0). Yields for 1 g precursor clay, calculated for $M^{II}_{1-x}Al_x(OH)_2(X^{n-})_{x/n}{\cdot}0.5H_2O$ where x = 0.36 for MgAl[Cl^-], 0.43 for ZnAl[NO_3^-], and the EDX-determined value for the polyoxometalate layered double hydroxides (Table 3): MgAl[$V_{10}O_{28}^{6-}$], 1.22 (75); MgAl[$V_2W_4O_{19}^{4-}$], 1.86 (90);

$MgAl[Nb_2W_4O_{19}^{4-}]$, 1.58 (70); $MgAl[Nb_3W_3O_{19}^{5-}]$, 1.39 (75); $MgAl[Nb_4W_2O_{19}^{6-}]$, 1.67 (102); $MgAl[Ti_2W_{10}PO_{40}^{7-}]$, 2.36 (96); $MgAl[HV_4W_8PO_{40}^{6-}]$, 2.36 (93); $ZnAl[Ti_2W_{10}PO_{40}^{7-}]$, 1.85 (86) and $ZnAl[NaP_5W_{30}O_{110}^{14-}]$, 2.43 g (90%).

The derivative $MgAl[V_2W_4O_{19}^{4-}]$ was also prepared *via* $MgAl[Br^-]$ in ethanol–dichloromethane. Thus, a $MgAl[NO_3^-]$ slurry (21 cm^3) containing clay (0.8 g) was stirred with NaBr (0.56 g, 6 mmol) for 1 d at 25 °C. After centrifuging, the supernatant was decanted off and the clay treated similarly with a fresh solution of NaBr (0.56 g) in decarbonated water (23 cm^3). The product was washed thoroughly with decarbonated water, ethanol and finally redispersed in ethanol (net weight in 10 cm^3 = 0.3 g). Infrared spectroscopy and XRD confirmed complete exchange for bromide (d_{003} = 7.88 Å). A solution of $Na_4[V_2W_4O_{19}]\cdot 14H_2O$ (3.11 g, 2 mmol) in decarbonated water (10 cm^3) was shaken for 15 min with a solution of NBu^n_4Br (5.42 g, 17 mmol) in dichloromethane (10 cm^3). The UV/VIS spectroscopic measurements indicated approximately 50% transfer of the polyoxometalate to the organic layer which was subsequently separated and dried with $MgSO_4$. The yellow-orange CH_2Cl_2 solution (7 cm^3) was then stirred with ethanolic $MgAl[Br^-]$ overnight at 25 °C. The product was isolated by centrifugation and washed with CH_2Cl_2–EtOH (1:1) followed by ethanol. The POXRD pattern showed three harmonics due to tungstovanadate-anion-pillared layered double hydroxide: 2θ = 7.32 (003), 14.73 (006) and 22.26° (009); d_{003} = 12.07 Å. A weak reflection at 2θ = 22.26° (7.91 Å) assignable to (003) of unexchanged starting material was also observed.

By direct synthesis. The procedure described by Narita *et al.*[12] for the direct synthesis of a $Zn_2Al[\alpha\text{-}SiW_{11}O_{39}^{8-}]$ layered double hydroxide was followed, with some modifications. The example which follows is for $ZnAl[NaP_5W_{30}O_{110}^{14-}]$.

A solution of $K_{12.5}Na_{1.5}[NaP_5W_{30}O_{110}]$ (1.16 g, 0.141 mmol) in deionised water (100 cm^3) was heated to 95–100 °C. To this were added dropwise simultaneously with stirring at 100 °C two solutions of $Zn(NO_3)_2\cdot 6H_2O$ (0.58 g, 1.95 mmol) and $Al(NO_3)_3\cdot 9H_2O$ (0.37 g, 0.986 mmol) in deionised water (15 cm^3) and 0.20 mol dm^{-3} NaOH (40 cm^3, 8 mmol). The addition rates were controlled in order to maintain the pH at 7.5–7.9. After complete addition the precipitate was aged for 1 h, washed by filtration with water and dried under reduced pressure at room temperature in a vacuum desiccator. The derivatives $ZnAl[Ti_2W_{10}PO_{40}^{7-}]$ (2.5 h and pH 7.6) and $MgAl[Nb_4W_2O_{19}^{6-}]$ (5 h and pH 9.6) were prepared in a similar manner.

From benzenecarboxylate-anion-pillared precursors. A series of organic-anion-pillared layered double hydroxides were prepared following the method first described by Drezdon.[7] A typical example follows (see Table 5 for sample identities, reaction conditions, and powder diffraction data). The net weight of clay in 25 cm^3 slurry was between 1.7 and 1.8 g for all products.

(*a*) $ZnAl[4\text{-}HOC_6H_4CO_2^-]$. A solution of $Zn(NO_3)_2\cdot 6H_2O$ (5.95 g, 20 mmol) and $Al(NO_3)_3\cdot 9H_2O$ (3.75 g, 10 mmol) in deionised water (30 cm^3) was added dropwise with vigorous stirring to a solution of 4-hydroxybenzoic acid (2.76 g, 20 mmol) and 50.2% NaOH (6.05 g, 79 mmol) in deionised water (60 cm^3). The precipitate was aged at 75 ± 3 °C for 2 d (pH 7.6), washed by filtration with deionised water and finally stored as an aqueous slurry.

(*b*) *Ion exchange.* A typical reaction scale was 40 cm^3 and involved the dropwise addition of a solution of the polyoxometalate in water to the precursor layered double hydroxide slurry (Table 1). The reaction mixtures were stirred for 1–2 h, at room temperature for $ZnCr[4\text{-}^-O_2CC_6H_4CO_2^-]$–$[V_{10}O_{28}^{6-}]$ and $NiAl[4\text{-}MeC_6H_4CO_2^-]$–$[V_2W_4O_{19}^{4-}]$, 60 °C for $ZnAl[4\text{-}HOC_6H_4CO_2^-]$–$[BW_{12}O_{40}^{5-}]$, 100 °C for $ZnAl[4\text{-}HOC_6H_4CO_2^-]$–$[SiW_{12}O_{40}^{4-}]$, 80–100 °C for $ZnAl[4\text{-}MeC_6H_4CO_2^-]$–$[HV_4W_8PO_{40}^{6-}]$ and 74 °C for $ZnAl[4\text{-}MeC_6H_4CO_2^-]$–$[PV_2W_{10}O_{40}^{5-}]$. In all cases the pH was controlled by addition of 2 mol dm^{-3} HNO_3. The work-up procedures differed according to the precursor benzenecarboxylate (see Results and Discussion section).

Acknowledgements

We thank the SERC (M. P.) for support, the Director of the Daresbury Laboratory for the provision of facilities, and Professor M. T. Weller for access to powder X-ray diffraction facilities.

References

1 A. Clearfield and M. Kuchenmeister, *ACS Symp. Ser.*, 1992, **499**, 128; S. L. Suib, *Chem. Rev.*, 1993, **93**, 803; T. J. Pinnavaia, *Science*, 1983, **220**, 365; F. Figueras, *Catal. Rev.-Sci. Eng.*, 1988, **30**, 457.
2 T. Kwon, G. A. Tsigdinos and T. J. Pinnavaia, *J. Am. Chem. Soc.*, 1988, **110**, 3653.
3 G. M. Woltermann, *US Pat.*, 4 454 244, 1984.
4 T. Tatsumi, K. Yamamoto, H. Tajima and H. Tominaga, *Chem. Lett.*, 1992, **5**, 815.
5 T. Kwon and T. J. Pinnavaia, *Chem. Mater.*, 1989, **1**, 381.
6 J. D. Wang, Y. Tian, R. C. Wang and A. Clearfield, *Chem. Mater.*, 1992, **4**, 1276.
7 M. A. Drezdon, *Inorg. Chem.*, 1988, **27**, 4628; *ACS Symp. Ser.*, 1990, **437**, 140.
8 K. Chibwe and W. Jones, *Chem. Mater.*, 1989, **1**, 489.
9 M.-A. Ulibarri, F. M. Labajos, V. Rives, R. Trujillano, W. Kagunya and W. Jones, *Inorg. Chem.*, 1994, **33**, 2592.
10 F. Kooli, V. Rives and M. A. Ulibarri, *Inorg. Chem.*, 1995, **34**, 5114; 5122.
11 E. D. Dimotakis and T. J. Pinnavaia, *Inorg. Chem.*, 1990, **29**, 2393.
12 E. Narita, P. D. Kaviratna and T. J. Pinnavaia, *J. Chem. Soc., Chem. Commun.*, 1993, 60.
13 J. Twu and P. K. Dutta, *J. Catal.*, 1990, **124**, 503; *Chem. Mater.*, 1992, **4**, 398.
14 E. L. Salinas and Y. Ono, *Bull. Chem. Soc. Jpn.*, 1992, **65**, 2465.
15 M. Doeuff, T. Kwon and T. J. Pinnavaia, *Synth. Met.*, 1989, **34**, 609.
16 J. F. Keggin, *Nature (London)*, 1933, **131**, 908; *Proc. R. Soc. London, Ser. A*, 1934, **144**, 75.
17 K. A. Carrado, A. Kostapapas and S. L. Suib, *Solid State Ionics*, 1988, **26**, 77; W. T. Reichle, *CHEMTECH*, 1986, 58; W. T. Reichle, *Solid State Ionics*, 1986, **22**, 135; W. Jones and M. Chibwe, in *Pillared Layered Structures*, Elsevier, Amsterdam, 1990, p. 67.
18 M. T. Pope, *Heteropolymetalates and Isopolymetalates*, Springer, Berlin, Heidelberg, 1983; M. T. Pope and A. Müller, *Angew. Chem., Int. Ed. Engl.*, 1991, **30**, 34.
19 J. M. Corker, J. Evans and J. M. Rummey, *Mater. Chem. Phys.*, 1991, **29**, 201; K. Bornholdt, J. M. Corker, J. Evans and J. M. Rummey, *Inorg. Chem.*, 1991, **30**, 1; J. F. W. Mosselmans, J. M. Corker, J. Evans, J. T. Gauntlett and J. M. Rummey, *Catal. Today*, 1991, **9**, 175.
20 A. De Roy, J. P. Besse and P. Bondot, *Mater. Res. Bull.*, 1985, **20**, 1091.
21 V. Rives, F. M. Labajos, M.-A. Ulibarri and P. Malet, *Inorg. Chem.*, 1993, **32**, 5000.
22 J. Evans, M. Pillinger and J. M. Rummey, *J. Chem. Soc., Dalton Trans.*, preceding paper.
23 C. Preyssler, *Bull. Soc. Chim. Fr.*, 1970, **1**, 30.
24 M. H. Alizadeh, S. P. Harmalker, Y. Jeannin, J. Martin-Frère and M. T. Pope, *J. Am. Chem. Soc.*, 1985, **107**, 2662.
25 D. M. Moore and R. C. Reynolds, *X-Ray Diffraction and the Identification and Analysis of Clay Minerals*, Oxford University Press, 1989.
26 N. N. Greenwood and A. Earnshaw, *Chemistry of the Elements*, Pergamon, Oxford, 1st edn., 1984, (*a*) ch. 23, pp. 1197–1199; (*b*) ch. 27, p. 1345.
27 Y. Dou, *J. Chem. Educ.*, 1990, **67**, 134.
28 F. M. Labajos, V. Rives and M. A. Ulibarri, *Spectrosc. Lett.*, 1991, **24**, 499.
29 W. Lowenstein, *Am. Miner.*, 1954, **39**, 92.
30 C. J. Serna, J. L. Rendon and J. E. Iglesias, *Clays Clay Miner.*, 1982, **30**, 180.
31 H.-P. Boehm, J. Steinle and C. Vieweger, *Angew. Chem., Int. Ed. Engl.*, 1977, **16**, 265.

32 G. W. Brindley and S. Kikkawa, *Am. Miner.*, 1979, **64**, 836.
33 M. J. Jaycock, in *Experiments in Physical Chemistry*, eds. J. M. Wilson, R. J. Newcombe, A. R. Denaro and R. M. W. Ricket, Pergamon, Oxford, 1962.
34 N. Binsted, PAXAS Program for the Analysis of X-Ray Absorption Spectra, University of Southampton, 1988.
35 S. J. Gurman, N. Binsted and I. Ross, *J. Phys. C*, 1984, **17**, 143; 1986, **19**, 1845.
36 M. Filowitz, R. K. C. Ho, W. G. Klemperer and W. Shum, *Inorg. Chem.*, 1979, **18**, 93.
37 C. M. Flynn and M. T. Pope, *Inorg. Chem.*, 1971, **10**, 2524.
38 M. Dabbabi and M. Boyer, *J. Inorg. Nucl. Chem.*, 1976, **38**, 1011.
39 G. K. Johnson and R. K. Murmann, *Inorg. Synth.*, 1979, **19**, 140.
40 Y. Jeannin and J. Martin-Frère, *Inorg. Synth.*, 1990, **27**, 93.
41 C. Rocchiccioli-Deltcheff, M. Fournier, R. Franck and R. Thouvenot, *Inorg. Chem.*, 1983, **22**, 207.
42 P. J. Domaille and W. H. Knoth, *Inorg. Chem.*, 1983, **22**, 818.
43 P. J. Domaille, *J. Am. Chem. Soc.*, 1984, **106**, 7677.
44 D. P. Smith and M. T. Pope, *Inorg. Chem.*, 1973, **12**, 331.
45 I. Creaser, M. C. Heckel, R. J. Neitz and M. T. Pope, *Inorg. Chem.*, 1993, **32**, 1573.
46 C. Rocchiccioli-Deltcheff, R. Thouvenot and M. Dabbabi, *Spectrochim. Acta, Part A*, 1977, **33**, 143; J. Fuchs, S. Mahjour and R. Palm, *Z. Naturforsch., Teil B*, 1976, **31**, 544.
47 W. T. Reichle, *J. Catal.*, 1985, **94**, 547; M. Meyn, K. Beneke and G. Lagaly, *Inorg. Chem.*, 1990, **29**, 5201.

Received 11*th January* 1996; *Paper* 6/00221H